




Research article

Influence of Anisotropy on Thermal Management in an Unconsolidated Porous Energy Storage Cavity

Chunyang Wang¹, Moghtada Mobedi², Xiao Yang¹, Yanan Shen¹, Haibo Zhao^{1,4}, Yujie Xu^{1,4}, Haisheng Chen^{1,3,4}, Ting Zhang^{1,3,4,5*}, Xinghua Zheng^{1,3,4,5*}

¹ Institute of Engineering Thermophysics, Chinese Academy of Sciences, Beijing 100190, China

² Mechanical Engineering Department, Faculty of Engineering, Shizuoka University, Hamamatsu-shi, 432-8561, Japan

³ Nanjing Institute of Future Energy System, Nanjing 211135, China

⁴ University of Chinese Academy of Sciences, Beijing 100049, China

⁵ University of Chinese Academy of Sciences, Nanjing, 211135, China

Keywords:

Underground energy storage
thermal management
gradient porosity
heat transfer
porous media

Cited as:

Wang CY, Mobedi M, Yang X, et al. 2025. Influence of Anisotropy on Thermal Management in an Unconsolidated Porous Energy Storage Cavity. *GeoStorage*, 1(2), 158-170.
<https://doi.org/10.46690/gS.2025.02.05>

Abstract:

Heat transfer in porous media is a core technical component for thermal management in underground energy storage systems. In this study, the anisotropy effect of unconsolidated porous media on thermal management within a cavity is numerically investigated. The research considers gradient porosity (ranging from 0.05 to 0.95) in different directions, under both pure conduction and natural convection conditions. The velocity and temperature distributions throughout the entire cavity are analyzed for various anisotropy gradients in different directions, with special attention paid to the temperature variation on the hot surface subjected to a constant heat flux. To characterize the temperature variation on the hot surface, two dimensionless parameters are defined: the variance of dimensionless temperature and temperature intensity (I_{\max} , I_{\min}). The obtained results indicate that for two-directional gradient porosity cases under natural convection, the largest difference ratio of variance is 40.9%, while the maximum difference ratios of I_{\max} and I_{\min} are 92.3% and 83.3%, respectively. For pure conduction cases, the largest difference ratios of variance, I_{\max} , and I_{\min} are 52.4%, 41.2%, and 75%, respectively. These results demonstrate that natural convection exerts a more significant influence on the heat transfer behavior. By arranging the anisotropy gradient in different directions, the temperature distribution on the hot surface can be adjusted as required. This finding is valuable for applications that demand a non-uniform temperature distribution.

1 Introduction

Underground energy storage, as a key technology for balancing the temporal and spatial mismatch between energy supply and demand and enhancing the integration of renewable energy, has attracted extensive attention in recent years (Liu et al., 2025). Its core principle is to use subsurface geological formations such as aquifers, rock layers, or salt caverns as storage space, in which thermal energy or electricity-derived converted energy (such as compressed air) is stored in specific forms within underground spaces, enabling large-scale, long-duration, and seasonal energy regulation.

In underground energy storage systems, thermal management is a central technical component that directly affects system efficiency, safety, and economic performance. Thermal management not only concerns temperature control during the energy storage process, but also involves the thermal interactions between the reservoir and surrounding geological formations, fluid flow and heat exchange efficiency, and the long-term operational behavior of the system. Recently the use of high conductive porous media (such as metal foam or lattice

metal frames) has taken the attentions of researchers (Wang and Mobedi, 2020). High conductive porous media increases the effective thermal conductivity of the flow field as well as mix the flow causing the considerable enhanced heat transfer between a base surface and fluid. There are many applications of heat transfer enhancement in industry in which the use of porous media can be suggested as the accelerating phase change process of energy storage (Tayebi et al., 2025; Ghalambaz et al., 2022), enhanced heat transfer in pipes (Zhang et al., 2024; Liu et al., 2024) and battery (Li et al., 2024; Mohammadi and Taghilou, 2024).

A porous medium includes voids and solid phase, and it can be classified into consolidated and unconsolidated porous media according the solid domain which is interconnected or unconnected with each other. Although practically consolidated heat transfer is widely used for heat transfer enhancement, unconsolidated porous media is widely used to develop theories and discover heat transfer and fluid flow behavior in a porous media. For instance, Reji et al. performed a numerical study on natural convection in a square cavity with adiabatic horizontal walls, thermally active vertical walls and containing blocks (Raji et al., 2012). The effects of Rayleigh number, thermal conductivity ratio and number of blocks were investigated. They found that the heat transfer and the flow intensity could be significantly reduced by increasing the number of the blocks and their relative thermal conductivity. Mansouri et al. conducted a study on natural convection flows and heat transfer characteristics in a square cavity confining conducting solid (Mansouri et al., 2020). The solid blocks resulting from the subdivision of the initial block are uniformly distributed within the cavity to maintain unchanged the volume occupied by the fluid. The obtained results showed that the block leads to heat transfer reduction between the thermally active walls of the cavity with negligible, moderate and important rates depending on the number of the blocks and the value of Rayleigh number. Ren et al. carried out research to simulate the transient process of natural convection in an enclosure with solid obstacles using Lattice Boltzmann Method (LBM) (Ren and Chan, 2016). They found that when more blocks are in the enclosure, the restriction on the convection due to the solid obstacles are stronger so that the Nusselt numbers become smaller. Hu et al. presented the effect of two configurations as disconnected and conducting solid obstacles on the natural laminar convection in a vertical enclosure numerically and analytically (Hu et al., 2016). They stated that the low thermal resistance of solid region reveals that solid obstacles could enhance the heat transfer process of both enclosures. Braga and Lemos studied heat transfer characteristics across a square cavity partially filled with a fixed amount of conducting solid materials, and the results showed that the average Nusselt number for cylindrical rods are slightly lower than those for square rods (Braga and de Lemos, 2005). Merrikh and Lage perfumed a study on natural convection in an enclosure with disconnected and conducting solid blocks, and they found that the overall heat transfer process can be enhanced by increasing solid-to-fluid conductivity ratio (Merrikh and Lage, 2005). Generally, although there are many literatures involving with fluid flow and heat transfer in high thermal conductive

unconsolidated porous media, there are relatively few studies on the gradient porosity of high thermal conductive unconsolidated porous media in the context of temperature control applications, and there is also a lack of in-depth research on the influence of high thermal conductive unconsolidated porous media on the heat conduction path and overall heat conduction.

In addition, some studies on the gradient porous media for enhancing heat transfer are reported in literature. Most of the studied porous media are consolidated porous media. For instance, Liu et al. conducted a study on the influence of non-uniform metal foams on heat transfer during phase transition by experiment and numerical simulation, and the results indicated the melting of PCM can be accelerated (Liu et al., 2023). Iasiello et al. investigated the effects of variable porosity and cell size on the thermal performance of functionally-graded foams, and they found that account for both variable porosity and cell size in metal foam can enhance Performance Evaluation Criteria (Iasiello et al., 2021). Jadhav et al. explored the use of partially filled high porosity graded aluminum and copper foams to satisfy both heat transfer and pressure drop in a heat exchanger, and the results revealed the graded metal foam can enhance heat transfer rate (Jadhav et al., 2021). Cheng et al. investigated transpiration cooling with phase change by functionally graded porous media, and the experimental results showed that the graded porous media exhibited much better cooling performance than uniform pore topology (Cheng et al., 2023). Based on the studies above, it can be seen the unconsolidated porous media has many advantages in the heat transfer fields. However, the research on heat transfer in gradient porosity structures mainly focuses on consolidated porous structures, while there is relatively less research on heat transfer in three-dimensional unconsolidated porous media.

Herein, the heat and fluid flow in a cavity assisted with unconsolidated porous media as square block can be accepted as fundamental case for investigating the roles of different parameters on heat and fluid flow. That is why this domain is used in this study to investigate the anisotropy effect of unconsolidated porous media on heat transfer through the cavity and to reveal the mechanism of thermal management by using gradient porous media. The aims of the current study are (a) to find parameters to define the temperature distribution of hot surface by using gradient porosity on the different direction, (b) to investigate and compare the mechanism of heat transfer for the gradient porosity on one and two directions.

2 Methodology

2.1 Physical model

The schematic view of the physical model is shown in Fig.1. A square cavity consists of unconsolidated porous media and working fluid, and the length of cubic cavity is equal to 16 mm. The porous media is a cubic cavity consisted of 512 solid blocks. All surfaces of the cavity are insulated except the right and left vertical surfaces are maintained at constant heat flux ($q = 10000 \text{ W/m}^2$) and constant temperature ($T_w = 293.15 \text{ K}$), respectively. The working fluid is air and the solid blocks are aluminum. The study was performed for 8 different cases of anisotropic porous media for two cases as pure conduction and

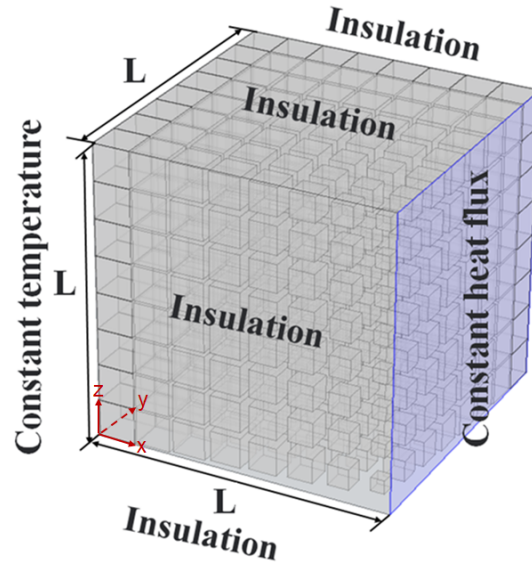


Fig. 1 The schematic view of physical model

Tab. 1 The values of the dimensionless coefficients for a_i and b_i

Gradients	a_i	b_i
Gradient 1 (Porosity: 0.05 0.95)	6.43	-0.0143
Gradient 2 (Porosity: 0.05 0.82)	5.51	-0.00511
Gradient 3 (Porosity: 0.05 0.69)	4.59	0.00407
Gradient 4 (Porosity: 0.05 0.56)	3.67	0.0133
Gradient 5 (Porosity: 0.05 0.44)	2.76	0.0224
Gradient 6 (Porosity: 0.05 0.31)	1.84	0.0316
Gradient 7 (Porosity: 0.05 0.18)	0.92	0.0408
Gradient 8 (Porosity: 0.05 0.05)	0	0

Tab. 2 The thermophysical properties of the considered materials (Wang et al., 2019)

Parameters	Air	Aluminum
Density (Kg/m ³)	1.177	2707
Thermal Conductivity (W/m K)	0.02623	204
Specific Heat Capacity (J/kg K)	1007	896

natural convection. Moreover, for natural convection problem the gravity affects in $-z$ direction and Boussinesq approximation is employed to include the buoyancy effect. The gradient porosity are applied in x , y and z direction, and this change is a linear change in the present study and it can be formulized by a line equation as Eq.1. In this equation, x , y and z show horizontal axis and vertical axis, and the dimensionless coefficient of a_i and b_i are tabulated in Tab.1. The porosity changes based on the values of a_i and b_i . The highest slope is for Gradient 1 while Gradient 8 has zero gradient (uniform block size). Additionally, the thermophysical properties of the considered materials are shown in Tab.2.

$$\varepsilon = a_i \eta + b_i \quad (1)$$

where η shows the center position of each cell in the directions which can be x , y and z . ε represents porosity, and can be calculated by $\frac{V_{\text{block}}}{V_{\text{control}}}$ for each block. V_{block} is the volume of the solid block, and V_{control} is the control volume. The number of the control volume is 512, and the sizes of the control volume

also are same. By changing the values of a_i and b_i , it is possible to adjust the gradient of the porosity in requested direction.

2.2 Governing equations

For the governing equations of natural convection case, the dimensional governing equations are presented, and the obtained results under steady state are given. In the present study, it is assumed that the thermophysical properties of porous media and working fluid are constant. The radiation effect is omitted. Based on the above assumption, the continuity, momentum and energy equations are presented in this section. The dimensional form of the governing equations can be written (Wang et al., 2019, 2022),

$$\nabla \cdot \mathbf{V} = 0 \quad (2)$$

$$(\mathbf{V} \cdot \nabla) \mathbf{V} = -\frac{1}{\rho_f} \nabla P + \nu_f \nabla^2 \mathbf{V} + g\beta(T - T_{ref})\mathbf{j} \quad (3)$$

$$(\rho C_p)_f (\mathbf{V} \cdot \nabla T_f) = k_f \nabla^2 T_f \quad (4)$$

$$0 = k_s \nabla^2 T_s \quad (5)$$

where β and T_{ref} are the volumetric thermal expansion coefficient of working fluid and reference temperature, respectively. The reference temperature is equal to the initial temperature and cold wall temperature in this study. C_p and k are heat capacity and thermal conductivity.

In the case of pure conduction, there is no natural convection, which means the velocity of fluid is zero. Therefore, only heat conduction equations exist.

$$0 = k_f \nabla^2 T_f \quad (6)$$

$$0 = k_s \nabla^2 T_s \quad (7)$$

2.3 Boundary conditions

A no-slip boundary condition is applied onto the top, bottom, front and back sides of the cavity, which are also thermally insulated, while the left wall is maintained at a constant temperature. A constant heat flux is imposed on the right wall of the cavity. The dimensional initial and boundary conditions are specified as follows:

$$\begin{cases} x = 0, 0 \leq y \leq L, 0 \leq z \leq L, & T = T_w, u = v = w = 0 \\ x = L, 0 \leq y \leq L, 0 \leq z \leq L, & q = q_w, u = v = w = 0 \\ 0 \leq x \leq L, y = 0, y = L, 0 \leq z \leq L, & \frac{\partial T}{\partial y} = 0 \\ 0 \leq x \leq L, y = 0, y = L, 0 \leq z \leq L, & \frac{\partial T}{\partial z} = 0 \end{cases} \quad (8)$$

For the interfacial boundary conditions between the solid blocks and fluid, the following continuity relations hold:

$$\frac{\partial T_s}{\partial n} = \frac{k_f}{k_s} \frac{\partial T_f}{\partial n}, T_f = T_s, V = 0 \quad (9)$$

where x, y, z are Cartesian coordinate axes, and \mathbf{n} is the unit vector normal to the interface surface.

3 Solution method and validation

In this study, the simulation of heat transfer process in an unconsolidated porous medium and the governing equations are solved by a software which uses the Finite Element Method. To validate the number of mesh, the mesh independency is done and shown in Fig. 2(a). Fig. 2(a) indicates the average temperature of the right vertical surface of the cavity for pure conduction case when the uniform porosity as 0.5 exist in each direction. The computational results for the five different number of elements are presented in Tab. 3. As it can be seen, the results of total 560864 and 918717 elements are same each

other which means the total 560864 elements are sufficient to obtain the accurate results, and can be used for saving computational period. For the convergence and tolerance criteria, it is automatically adjusted according to the software for calculating the accurate results.

Furthermore, a comparison between our numerical result and result of Merrikh and Lage reported in literature was done to validate the employed method and physical model in this study (Merrikh and Lage, 2005). The problem is an enclosure including a working fluid and several disconnect solid blocks distributed uniformly. The top and bottom walls are insulated while the right and left walls are given at a constant hot and cold temperature, respectively. Fig. 3(b) shows the comparison of the average Nusselt number between our numerical result and result of reference for various values of Raleigh number and two different values of solid block's number as 16 and 32 when the solid to fluid thermal conductivity ratio is equal to 1. It is observed that a good agreement between our numerical results and reported results of Merrikh and Lage exist, which reveals the employed method and physical model of the present study are correct (Merrikh and Lage, 2005). As it was mentioned before, a constant heat flux is applied onto the hot surface and the aim is to investigate the effect of anisotropy directions on temperature of the hot surface. To evaluate the temperature distribution of hot surface by using gradient porosity on two parameters are defined in the presented study, which are the variance of dimensionless temperature and the intensity of maximum temperature and minimum temperature changes. The variance of temperature change is to evaluate the dispersion degree of temperature change of hot surface, while the intensities of maximum and minimum temperature change are suggested to determine the intensity of temperature change. The definition of the first parameter is given,

The variance of the dimensionless temperature on the hot surface is defined as:

$$\text{Var}(\theta) = \frac{1}{n} \sum_{i=1}^n (\theta_i - \bar{\theta})^2 \quad (10)$$

where θ and $\bar{\theta}$ are the dimensionless temperature and its average on the hot surface, respectively. The dimensionless temperature is given by:

$$\theta = \frac{T - T_{\min}}{T_{\max} - T_{\min}} \quad (11)$$

The second parameters (intensity of minimum and maximum temperatures) are defined as:

$$I_{\max} = \frac{|T_{\max} - \bar{T}|}{\bar{T}} \quad (12)$$

$$I_{\min} = \frac{|T_{\min} - \bar{T}|}{\bar{T}} \quad (13)$$

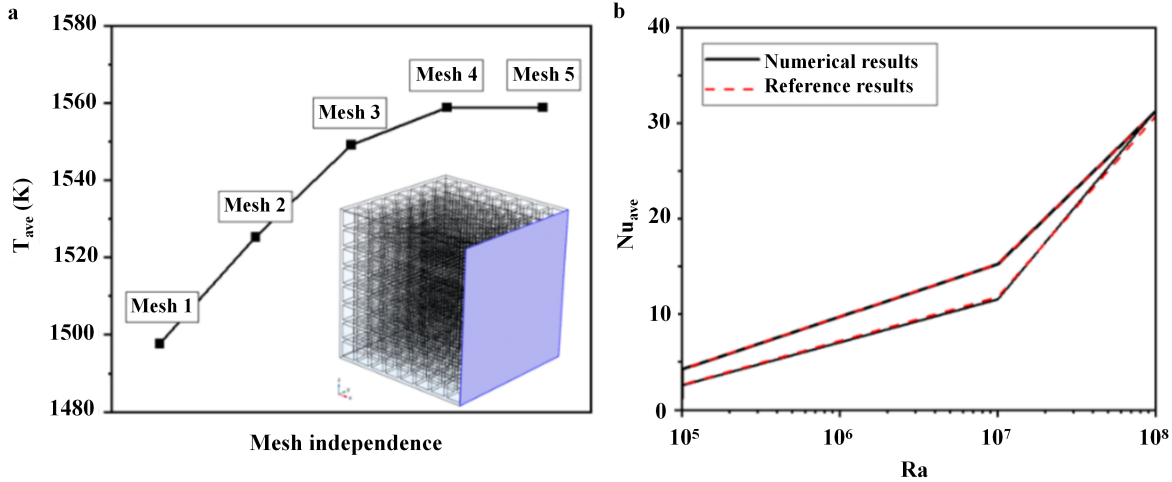


Fig. 2 The mesh independence and validation in this study, a: the comparison of the average temperature for the right vertical surface of cavity by using five different number of elements, b: the comparison results of the average Nusselt number between our numerical result and result of Merrikh and Lage (Merrikh and Lage, 2005) for two different values of the number of solid blocks

Tab. 3 The computational results for the five different number of elements

Parameter	Mesh 1	Mesh 2	Mesh 3	Mesh 4	Mesh 5
The number of elements	47294	80834	185575	560864	918717
T_{ave} (K)	1497.7	1525.3	1549.1	1558.8	1558.8

where the average dimensional temperature of the hot surface is:

$$\bar{T} = \frac{1}{n} \sum_{i=1}^n T_i \quad (14)$$

Here, T_{max} and T_{min} are the maximum and minimum dimensional temperatures of the hot surface, while \bar{T} is the average of the dimensional temperature of the hot surface.

4 Results and discussion

The study is done for two kinds of anisotropy as one directional anisotropy which is the gradient porosity only in one direction (such as porosity changes in x, y or z) and two directional anisotropies referring to change of porosity in two directions (such as porosity changes in (x, y) or (y, z) directions). The results of them are presented separately in this section. Furthermore, two cases as natural convection and pure conduction are investigated in this study. It must be mentioned that there is no contact between the cubic blocks and the walls, and a flow may exist not only between the blocks but also between the blocks and wall. This issue can be seen from Fig. 3. The non-uniform temperature distribution of cavity can be observed in the vertical direction, which indicates that air can flow between the blocks as well as block and the walls when the porosity is sufficiently large. The velocity vectors show the direction of fluid flow. This allows us to observe both the effect of buoyance and anisotropy on the hot surface.

4.1 The results of the gradient porosity in one direction

Fig.4 shows the temperature distributions for the gradient porosity of cavity under pure conduction when the applied heat flux is 10000 W/m^2 on the hot surface ($x = 16 \text{ mm}$). Positive direction means the gradient porosity in the cavity changes from the low porosity to the high porosity, while negative direction indicates the gradient porosity in cavity varies from the high porosity to the low porosity. Fig.4(a) illustrates the temperature distribution of solid blocks for positive and negative gradients in x, y and z directions. Temperature distribution on the hot surface is shown in Fig.4(b).

As shown in Fig.4(a), a uniform temperature change exists when the gradient porosity is only in x direction, due to the absence of porosity variation in the y and z directions and dominant conductive heat transfer with negligible fluid flow against gravity. The uniformity of temperature in y and z directions can also be seen from the blocks which are near the hot surface ($x = 16 \text{ mm}$). However, the situation is different when the porosity changes in y or z directions. Based on the direction of porosity change, there is an edge with maximum temperature and the temperature decreases towards the opposite corner almost linearly. Since the thermal conductivity of air is low which causes heat does not flow into other directions, the temperature rises near the edge occurs. In the other words, heat transfer in the region with high porosity near the edge is weak.

Temperature distribution on the hot surface presented in Fig.4(b) shows the thermal behavior clearly. With a gradient porosity in the x-direction, an approximately uniform (or peri-

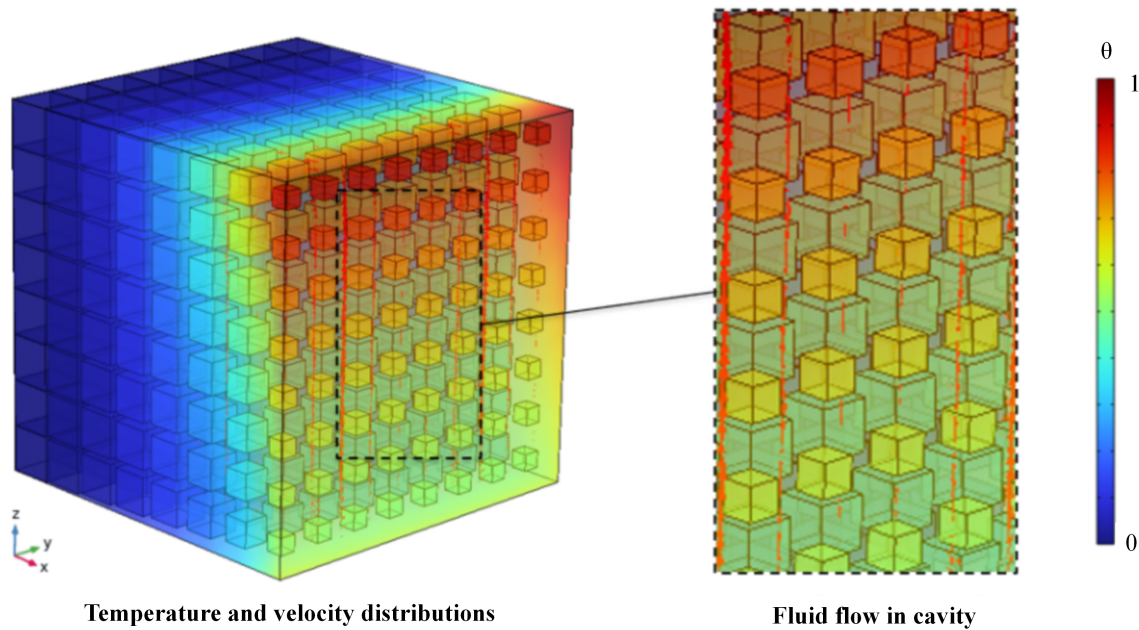


Fig. 3 Observation of flow between the solid blocks as well as solid blocks and hot surface

odic) temperature distribution is observed. In contrast, gradient porosity in the y or z directions result in edge-rise temperature distributions. Despite a uniform heat flux applied to the surface, a steep linear temperature gradient develops from one edge of the hot surface to the opposite edge. The reasons for the linear temperature change from one edge to opposite edge are the pure heat conduction in the cavity as well as anisotropy gradients in y or z directions.

Fig.5 shows the temperature distribution of solid blocks in the cavity and on the hot surface under natural convection. Since the effect of natural convection, the pattern of temperature on the hot surface changes considerably. For positive gradient porosity in x direction, the effect of natural convection near the hot surface can be seen easily. There is a sufficient void near the hot surface to have motion of fluid from bottom to top region due to natural convection. Conversely, for negative gradient porosity in x direction, there is no space near the hot surface and fluid cannot move. On the other word, region near the hot surface is not influenced by natural convection due to narrow interval volume and that's why a uniform temperature distribution is seen on the hot surface. For the case of gradient porosity in y direction, there are large free spaces on the region close to edges ($x = 16$ mm and $y = 16$ mm edge for positive gradient porosity change, and $x = 16$ mm and $y = 0$ edge for negative gradient porosity change) and hot fluid can be accumulated in the top corner due to natural convection. This fact can also be seen from the temperature distribution on the hot surface on which a heat flux is applied. The interesting result is the temperature distribution for the cavity with gradient porosity in z direction. The highest temperature is seen on the top and bottom edge regions in which a large space for the motion of fluid exists. The temperature for this case is similar to what obtained for the cavity with pure conduction heat transfer.

Fig.6 shows the comparison of variance on the hot surface for gradient porosity in each direction. Fig.6a presents the results of pure conduction case, while Fig.6b gives the results of natural convection case. As can be expected, the variances for the $\pm y$ and $\pm z$ directions are the same and the values are equal to 0.105, reflecting identical temperature changes despite different direction. For $\pm x$ directions, a different scenario presents itself. For the gradient porosity in $-x$ direction, a uniform temperature is observed on the hot surface while a periodical temperature distribution is observed for porous media with the gradient porosity in $+x$ direction due to the large free area around the hot surface. This causes the variance of temperature at $+x$ direction becomes larger than $-x$ direction as shown in Fig.6a, and the values of the variance of temperature are 0.008 and 0.0005, respectively. To observe the effect of natural convection on the temperature distribution on the hot surface, Fig.6b is prepared. Since the change is almost symmetry, the variances for $\pm y$ are same. For $\pm z$ directions, the variances are not same, the heated air can flow upward and increase the temperature of the blocks. For $+x$ direction, the hot air is accumulated on the top edge near the hot surface. The temperature change on the hot surface is small for $-x$ direction, however a high value of variance is seen since dimensionless temperature is considered to determine the variance. Compared to the values of the variance for the cases of the gradient porosity in y and z directions, the maximum difference for the case of the gradient porosity in x direction is 99.5%, which means the an almost uniform temperature distribution exists on the hot surface.

To observe the effect of natural convection on the temperature distribution on the hot surface, Fig.6b is prepared. Since the change is almost symmetry, the variances for $\pm y$ are same and equal to 0.055, which indicates the natural convection has the same effect on the hot surface. For the cases of the gradient

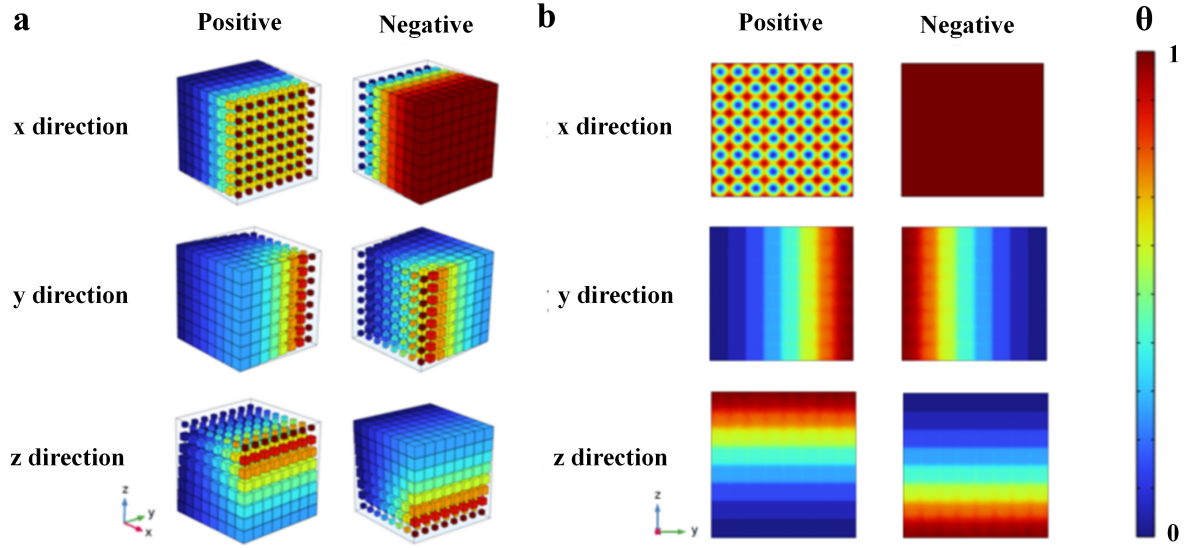


Fig. 4 Temperature distribution for the case of pure heat conduction for gradient porosity in different direction, a: temperature distribution of solid blocks, b: temperature distribution of hot surface

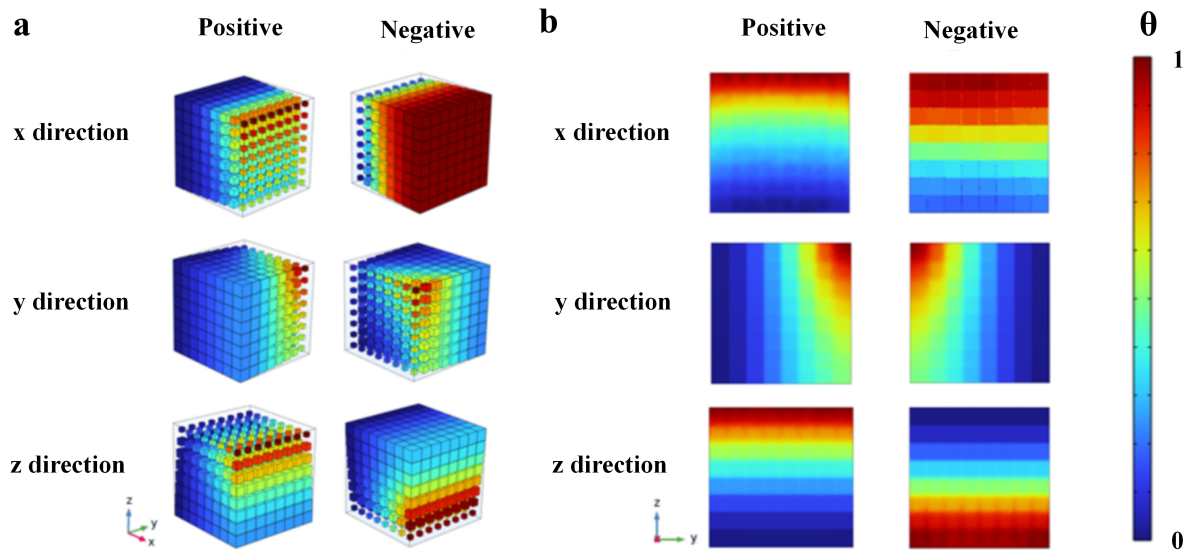


Fig. 5 Temperature distribution for cavity with natural convection for gradient porosity in different direction, a: temperature distribution of solid blocks, b: temperature distribution on the hot surface

porosity in $\pm z$ directions, the heated air can flow upward and increase the temperature of the solid blocks, while conduction is dominated in the region of low porosity near the hot surface. Hence, the temperature of low porosity region is lower than that of high porosity region. For the cases of the gradient porosity in $+x$ direction, there is big difference between natural convection and pure conduction cases. In the natural convection case, the hot air is accumulated on the top edge near the hot surface. And the temperature change on the hot surface is small for the case in $-x$ direction due to the low porosity near the hot surface. Since dimensionless temperature is considered to determine the variance, a high value of variance is seen and the value is close

to 0.08, which is 10 times greater than that of conduction case. Similarly, the effect of natural convection decreases the region of high temperature, which leads the values of variance reduce by 50% compared to pure conduction cases of gradient porosity in y direction.

As it was mentioned before, the variance is useful to determine the temperature change. To generalize the results in this study, it is possible to use the variance based on the dimensionless temperature. However, only variance does not provide details about the magnitude of dimensional change. Therefore, two parameters more are defined to describe the temperature change on the hot surface mathematically. Those parameters are

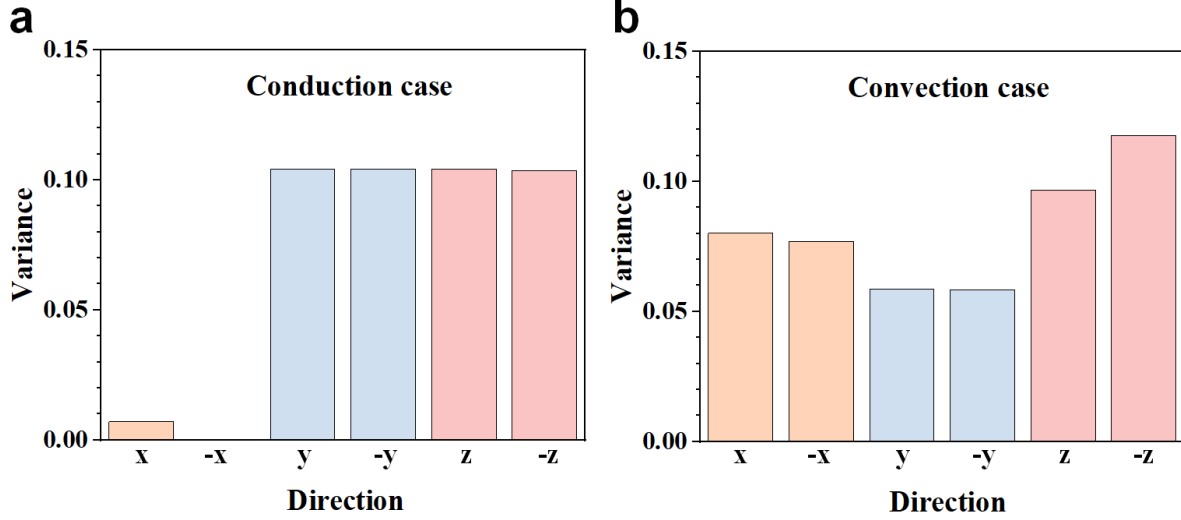


Fig. 6 The variance of dimensionless temperature on the hot surface for different one-dimensional gradient porosity, a: conduction heat transfer, b: convection heat transfer

maximum and minimum temperature intensity defined by Eqs. (12-13). Fig.7 shows the change of maximum and minimum temperature intensity on the hot surface for different directions of the gradient porosity and for the conduction and convection cases. In Fig.7a and Fig.7b which are plotted for conduction case, it is observed that the values of I_{\max} and I_{\min} are almost zero for the cases of gradient porosity in $\pm x$ directions. The variance is also small indicating that almost negligible temperature change for the cavities with the gradient porosity in $\pm x$ directions for conduction case.

And the values of I_{\max} are near 33% greater than that of I_{\min} for the cases of gradient porosity in $\pm y$ and $\pm z$ directions, which means the area of hot temperature region is also larger than that of low temperature region.

Fig.7c and 7d illustrate the variations of I_{\max} (maximum temperature intensity) and I_{\min} (minimum temperature intensity) for different gradient porosity configurations, considering the presence of natural convection in the cavity. Natural convection exerts a notable influence on the heat transfer behavior in the low-porosity region adjacent to the hot surface. Consequently, for the gradient porosity in the $+x$ direction, the values of I_{\max} and I_{\min} increase to 0.34 and 0.22, respectively, compared to the pure conduction cases. For gradient porosity in the $\pm y$ directions, the relatively high I_{\max} values indicate a significant temperature rise, which is correlated with the average temperature on the hot surface. As previously explained, due to the symmetry of temperature distribution, I_{\max} is identical for both $+y$ and $-y$ gradient porosity configurations. The natural convection effect contributes to the elevation of the hot region temperature. Additionally, I_{\min} for $\pm y$ directions is smaller than I_{\max} , implying that a steep high-temperature gradient exists in a limited area of the hot surface, while low temperatures dominate most of the hot surface.

Regarding gradient porosity in the $\pm z$ directions, I_{\max} is smaller than that in the $\pm y$ directions, indicating an expansion of the high-temperature area. This expansion is more pronounced for the $-z$ direction gradient porosity, where a wider region of

the hot surface exhibits high temperatures. For $\pm z$ configurations, I_{\max} and I_{\min} are relatively close, suggesting that the areas of high and low temperatures are spatially adjacent.

For the $-x$ direction gradient porosity, both I_{\max} and I_{\min} are extremely small, and the hot surface temperature is nearly uniform.

It should be noted that variance is calculated using dimensionless temperatures to facilitate comparisons between different cases. However, variance alone cannot provide accurate information about surface temperature characteristics. Only by considering both temperature intensity (I_{\max} , I_{\min}) and variance can a comprehensive and correct understanding of the surface temperature distribution be obtained.

4.2 The results of the gradient porosity in two directions

The temperatures of solid blocks in the cavity with two directional gradient porosity for pure conduction heat transfer are shown in Fig.8a. As can be seen, the gradient porosity changes in both directions of $(-x, -y)$, $(-x, -z)$, $(-x, z)$, $(x, -y)$, $(x, -z)$, (x, z) as well as $(+z, -y)$ and $(-z, -y)$. The temperature on the hot surface for all these cavities are also shown in Fig.8b. It is obvious that the temperature changes on the hot surface completely by changing gradient porosity in the different direction. The temperature distribution on the hot surface with gradient porosity in $-x$ direction is similar to each other, although the direction of temperature change is different. Similarly, the temperature change of solid blocks for the gradient porosity in $+x$ direction is similar, and the highest temperature occurs on an edge. Based on the direction of gradient porosity, the location of edge varies. For the no gradient porosity in x direction ($(+z, -y)$ and $(-z, -y)$), the higher temperature occurs on the corner based on the direction of gradient porosity. Generally, the temperature of the hot surface that is near the high porosity region is also higher, when the gradient porosity exists near the hot surface. For the uniform porosity close to the hot surface, when there is a steep gradient porosity in the heat transfer direction, the

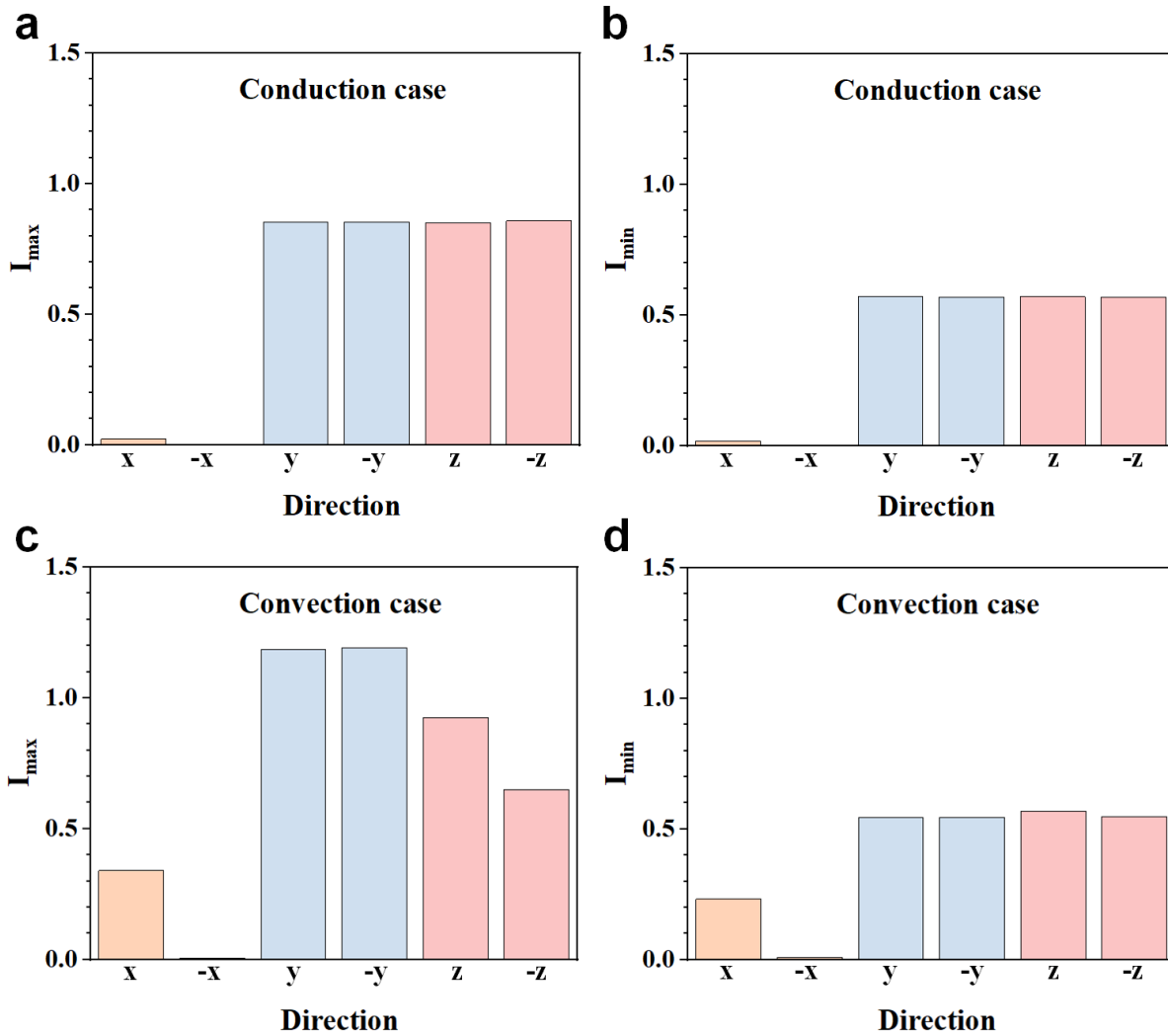


Fig. 7 The change of temperature intensity on the hot surface with porosity change direction, a-b: conduction heat transfer, c-d: convection heat transfer

region temperature is higher near the hot surface. Based on the temperature distributions, the heat transfer direction and behavior can be adjusted by changing the directions of the gradient porosity.

Fig.9 depicts the variations of variance, maximum temperature intensity (I_{\max}), and minimum temperature intensity (I_{\min}) across different two-directional gradient porosity cases.

Regardless of the temperature magnitude, the minimum variance is observed for the gradient porosity configurations in the $(+z, -y)$ and $(-z, -y)$ directions. It should be noted that the variance of dimensionless temperatures alone cannot provide a realistic reflection of the hot surface temperature changes; therefore, I_{\max} and I_{\min} must also be considered for comprehensive analysis.

The minimum I_{\max} values are found in the configurations with gradient porosity in the $(-x, -z)$, $(-x, +z)$, and $(+z, -y)$ directions. Voids are present on the back side of the cavity ($x = 0$), and conduction heat transfer dominates the region near the hot surface. Consequently, the temperature of the solid blocks increases over almost the entire hot surface. Both I_{\min}

and I_{\max} are low and of nearly the same order of magnitude, indicating that the hot surface temperature distribution is close to uniform.

For the gradient porosity configurations in the $(+x, -y)$, $(+x, -z)$, and $(+x, +z)$ directions, I_{\max} and I_{\min} increase by approximately the same amount, which implies a steeper temperature gradient on the hot surface. In contrast, for the two configurations $(+z, -y)$ and $(-z, -y)$, I_{\max} increases significantly while I_{\min} remains nearly unchanged compared to the $(+x, -y)$, $(+x, -z)$, and $(+x, +z)$ cases. These I_{\max} and I_{\min} characteristics correspond to a high temperature concentrated in a small region of the hot surface, while the remaining areas maintain a low temperature (as reflected by the small I_{\min} value).

Regarding the variance, the largest difference ratio between any two configurations is 52.4%, observed between the $(-z, -y)$ and $(-x, -z)$ gradient porosity cases. For I_{\max} and I_{\min} , the maximum difference ratios across different gradient porosity configurations are 41.2% and 75%, respectively.

Fig.10 illustrates the temperature distributions of solid blocks in the cavity and the hot surface for various gradient porosity

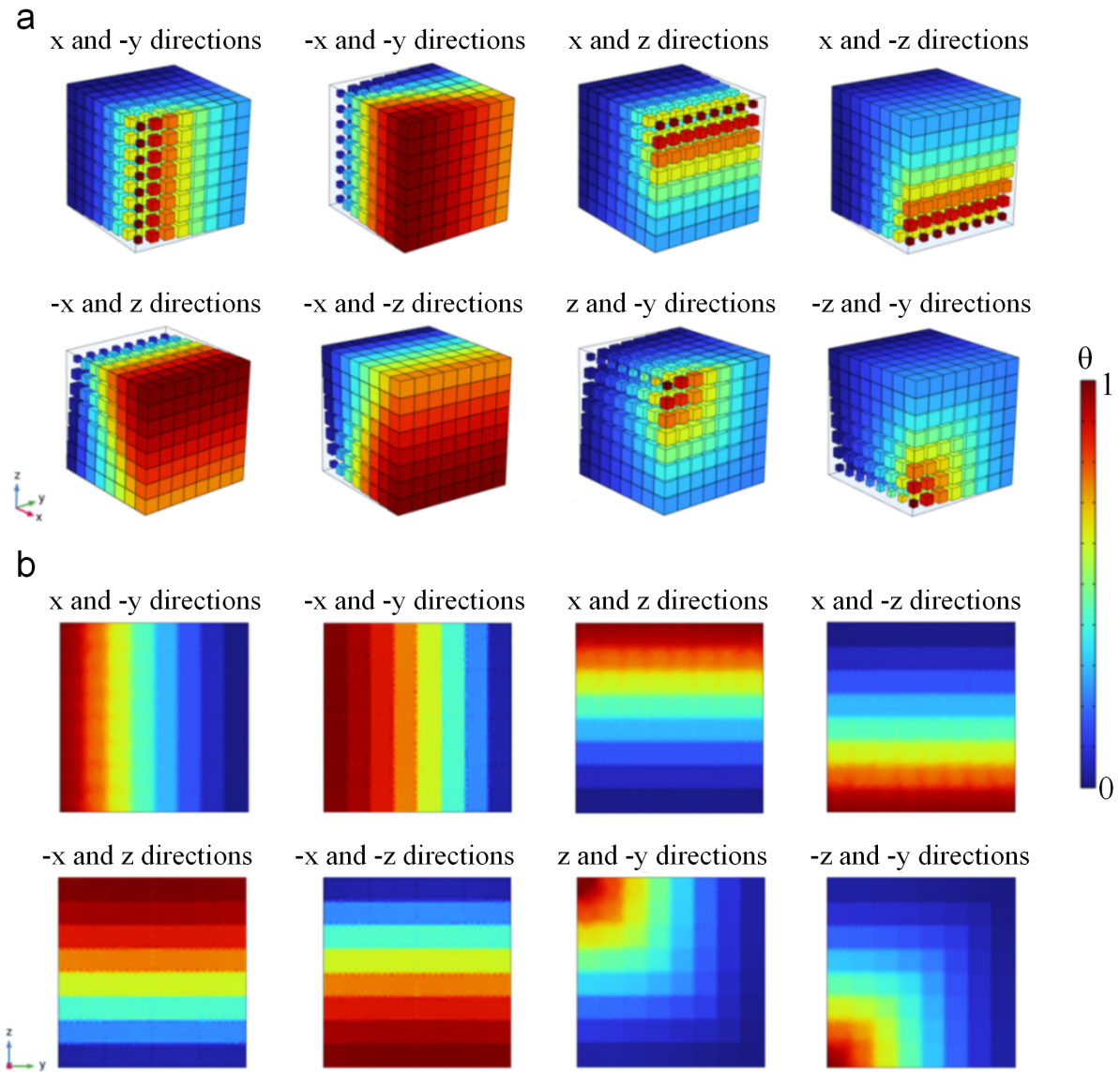


Fig. 8 Temperature distribution for the case of pure heat conduction for gradient porosity in two directions, a: temperature distribution of solid blocks, b: temperature distribution of hot surface

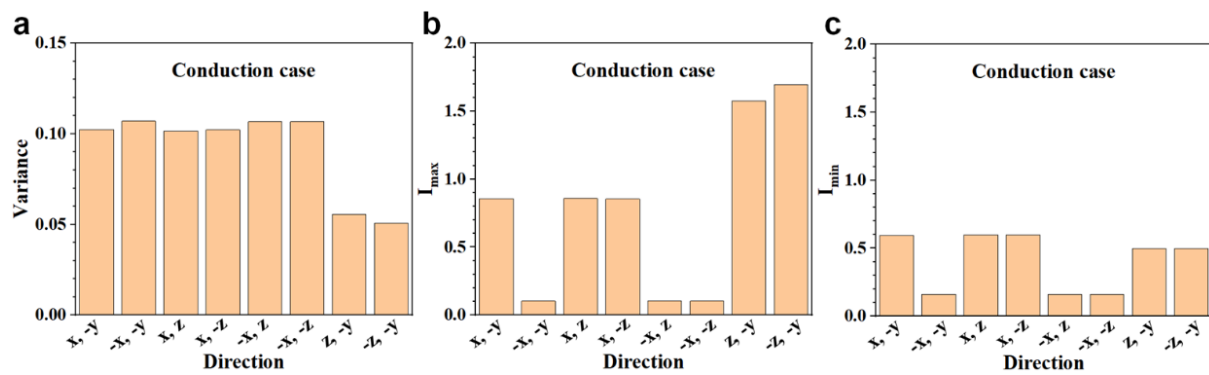


Fig. 9 The suggested parameters for specifying the change of temperature on the hot surface with gradient porosity in two directions for conduction heat transfer case, a: variance of dimensionless temperature, b: maximum temperature intensity, c: minimum temperature intensity

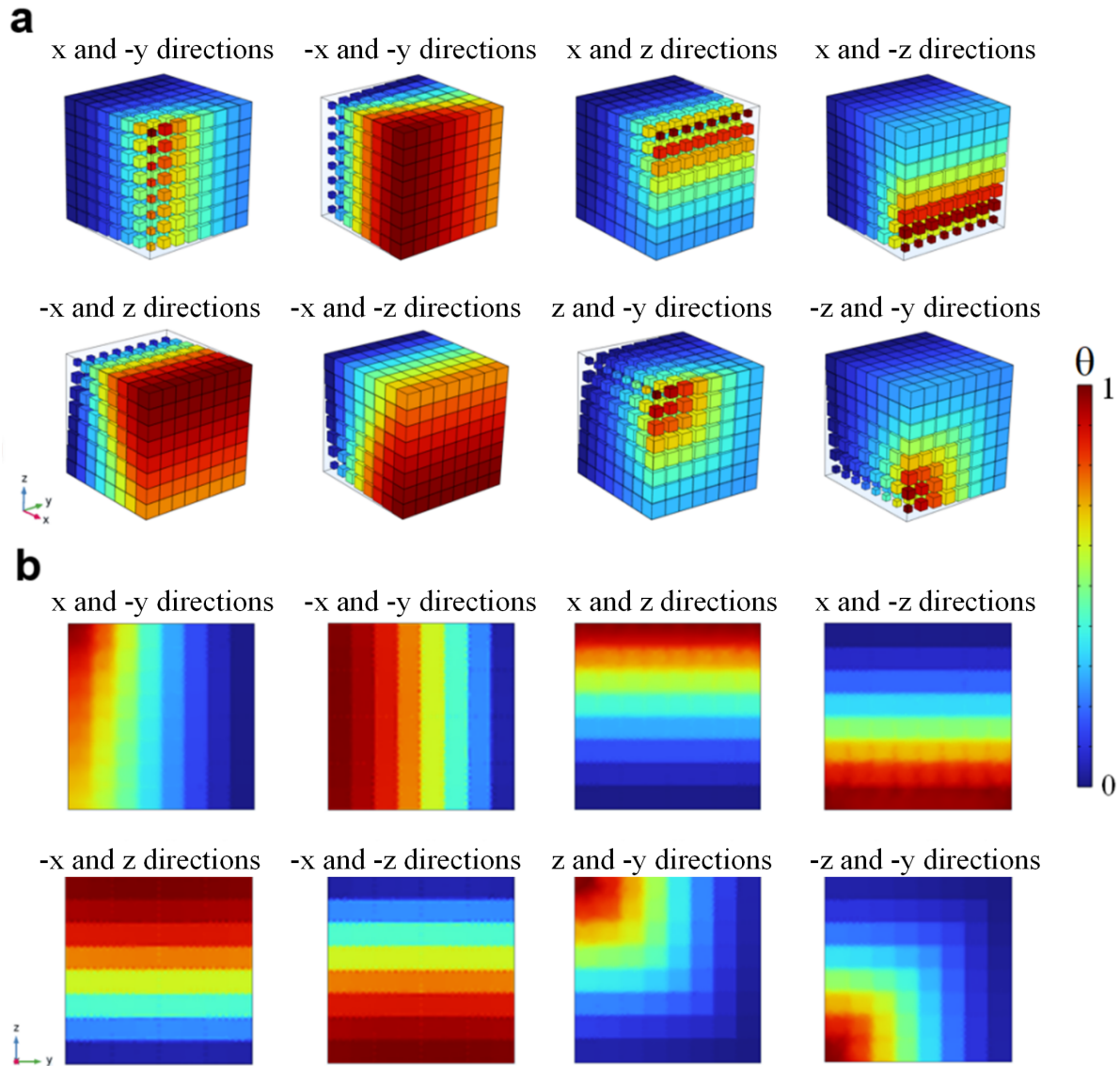


Fig. 10 Temperature distribution for the case of gradient porosity in two directions when natural convection exists, a: temperature distribution of solid blocks, b: temperature distribution of hot surface

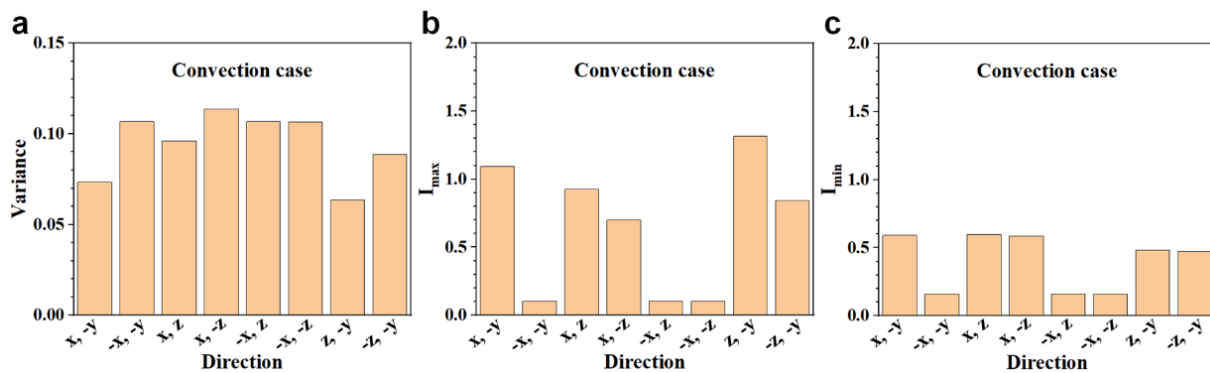


Fig. 11 The suggested parameters for specifying the change of temperature on the hot surface with gradient porosity in two directions for cavity with convection heat transfer case, a: variance of dimensionless temperature, b: maximum temperature intensity, c: minimum temperature intensity

configurations under natural convection conditions. Specifically, Fig.10a presents the temperature distribution of solid blocks for different gradient porosity cases, while Fig.10b shows the corresponding hot surface temperature distribution.

In general, the temperature distribution characteristics shown in Fig.10 (natural convection case) are similar to those in Fig.8 (pure conduction case). The primary difference lies in the temperature variation along the z -direction, indicating that natural convection exerts a significant influence on heat transfer in the z -direction.

For example, in the configuration with gradient porosity in the $(+x, -y)$ direction, a higher temperature is observed at the top corner of the solid blocks. This phenomenon is attributed to the upward movement of hot air flow driven by natural convection. However, for configurations where the low-porosity region is adjacent to the hot surface (e.g., gradient porosity in the $(-x, -y)$ and $(-x, -z)$ directions), the impact of natural convection becomes negligible.

Fig.11 presents the variations of the variance of dimensionless temperature, maximum temperature intensity (I_{\max}), and minimum temperature intensity (I_{\min}) for the cavity under natural convection conditions.

For the same gradient porosity configurations (with different directions), the variations of these parameters are very close to those in the pure conduction case. Although slight numerical changes can be observed, the overall variation trends remain consistent. However, the most significant changes in variance and I_{\max} are found for the gradient porosity configuration in the $(-z, -y)$ direction. In this case, large voids are located at the bottom corner of the cavity: as the air temperature rises, the hot air ascends and distributes heat more extensively throughout the cavity compared to pure conductive heat transfer. This explains why the variance and I_{\max} values are lower than those in the pure conduction case.

Regarding the variance, the largest difference ratio between any two gradient porosity configurations is 40.9%, observed between the $(z, -y)$ and $(x, -z)$ directions. For I_{\max} and I_{\min} , the maximum difference ratios across different configurations are 92.3% and 83.3%, respectively. These results indicate that natural convection plays a crucial role in regulating the heat transfer behavior of the cavity.

5 Conclusions

In this study, the impact of anisotropy on the thermal management of a cavity containing an unconsolidated porous structure is numerically investigated. The research is conducted for both natural convection and pure conduction scenarios, with the following objectives:

- Develop a solution method for evaluating the hot surface temperature distribution by adjusting gradient porosity in different directions;
- Investigate and compare the heat transfer mechanisms of one-directional and two-directional gradient porosity;
- Compare and discuss three key parameters: variance of dimensionless temperature, temperature intensity (I_{\max} , I_{\min}), and the area ratio of temperature regions on the hot surface.

For future work, the same investigation should be extended to three-directional gradient porosity configurations. Additionally, more critical parameters and their correlations for controlling temperature distribution need to be identified and analyzed.

Based on the obtained results and detailed discussions, the following conclusions are drawn:

- Generally, gradient porosity and its direction exert a significant influence on the temperature distribution. Specifically, the temperature in high-porosity regions is relatively high, while low-porosity regions exhibit lower temperatures. Furthermore, natural convection can enhance the non-uniformity of temperature distributions for solid blocks and the hot surface in the case of one-directional gradient porosity.
- For one-directional gradient porosity configurations: although the variance and temperature intensity values on the hot surface are smaller for gradient porosity in the x and $-x$ directions, the area difference between low-temperature and high-temperature regions is more pronounced.
- Compared with one-directional gradient porosity results, natural convection plays a negligible role in the temperature distributions of solid blocks and the hot surface, except for the gradient porosity configurations involving the x and $-y$ directions.
- For the same gradient porosity directions, the variation trends of variance and temperature intensity on the hot surface are consistent between natural convection and pure conduction scenarios.

Acknowledgements

This work was supported by the National Key Research and Development Program of China (2023YFB3809800), the National Natural Science Foundation of China (No. 52525601, No.52172249), the Scientific Instrument Developing Project of the Chinese Academy of Sciences (P-TYQ2025TD0018), the Chinese Academy of Sciences Talents Program (E2290701), the Special Fund Project of Carbon Peaking Carbon Neutrality Science and Technology Innovation of Jiangsu Province (BE2022011) and Basic Research Program of Jiangsu (BK20251714).

Conflict of interest

The authors declare no competing interest.

Open Access This article is distributed under the terms and conditions of the Creative Commons Attribution (CC BY-NC-ND) license, which permits unrestricted use, distribution, and reproduction in any medium, provided the original work is properly cited.

References

- Braga EJ, de Lemos MJ S. 2005. Heat transfer in enclosures having a fixed amount of solid material simulated with heterogeneous and homogeneous models. *International Journal of Heat and Mass Transfer*, **48**: 4748–4765. doi:10.1016/j.ijheatmasstransfer.2005.05.016.
- Cheng ZL, Xu RN, Jiang PX. 2023. Transpiration cooling with phase change by functionally graded porous media. *International Journal of Heat and Mass Transfer*, **205**: 123862. doi:10.1016/j.ijheatmasstransfer.2023.123862.

- Ghalambaz M, Melaibari AA, Chamkha AJ, Younis O, Sheremet M. 2022. Phase change heat transfer and energy storage in a wavy-tube thermal storage unit filled with a nano-enhanced phase change material and metal foams. *Journal of Energy Storage*, **54**: 105277. doi:10.1016/j.est.2022.105277.
- Hu JT, Ren XH, Liu D, Zhao FY, et al. 2016. Conjugate natural convection inside a vertical enclosure with solid obstacles of unique volume and multiple morphologies. *International Journal of Heat and Mass Transfer*, **95**: 1096–1114. doi:10.1016/j.jheatmasstransfer.2015.12.070.
- Iasiello M, Bianco N, Chiu WKS, et al. 2021. The effects of variable porosity and cell size on the thermal performance of functionally-graded foams. *International Journal of Thermal Sciences*, **160**: 106696. doi:10.1016/j.ijthermalsci.2020.106696.
- Jadhav PH, Gnanasekaran N, Perumal DA, et al. 2021. Performance evaluation of partially filled high porosity metal foam configurations in a pipe. *Applied Thermal Engineering*, **194**: 117081. doi:10.1016/j.applthermaleng.2021.117081.
- Li B, Zhang L, Shang B, et al. 2024. Numerical investigation on heat transfer characteristics in battery thermal management with phase change material composed by toroidal porous medium. *International Communications in Heat and Mass Transfer*, **154**: 107414. doi:10.1016/j.icheatmasstransfer.2024.107414.
- Liu G, Xiao T, Wei P, et al. 2023. Experimental and numerical studies on melting/solidification of PCM in a horizontal tank filled with graded metal foam. *Solar Energy Materials and Solar Cells*, **250**: 112092. doi:10.1016/j.solmat.2022.112092.
- Liu JJ, Yang CH, Song R, et al. 2025. Advances of Geological Storage Engineering and Technology. *GeoStorage*, **1**(1): 1–26. doi:10.46690/gst.2025.01.01.
- Liu Y, Chen CW, Wang JT, et al. 2024. Experimental study on the heat transfer characteristics of a novel self-driven cooling system. *International Journal of Heat and Mass Transfer*, **221**: 125085. doi:10.1016/j.jheatmasstransfer.2023.125085.
- Mansouri AE, Hasnaoui M, Amahmid A, Alouah M. 2020. Numerical analysis of conjugate convection-conduction heat transfer in an air-filled cavity with a rhombus conducting block subjected to subdivision: Cooperating and opposing roles. *International Journal of Heat and Mass Transfer*, **150**: 119375. doi:10.1016/j.jheatmasstransfer.2020.119375.
- Mohammadi MS, Taghilou M. 2024. Thermal investigation of a lithium-ion cell in presence of PCM within the porous medium considering local thermal nonequilibrium condition. *Journal of Energy Storage*, **86**: 111205. doi:10.1016/j.est.2024.111205.
- Merrikh AA, Lage JL. 2005. Natural convection in an enclosure with disconnected and conducting solid blocks. *International Journal of Heat and Mass Transfer*, **48**: 1361–1372. doi:10.1016/j.jheatmasstransfer.2004.09.043.
- Raji A, Hasnaoui M, Naimi M, Slimani K, Ouazzani MT. 2012. Effect of the subdivision of an obstacle on the natural convection heat transfer in a square cavity. *Computers and Fluids*, **68**: 1–15. doi:10.1016/j.compfluid.2012.07.014.
- Ren QL, Chan CL. 2016. Natural convection with an array of solid obstacles in an enclosure by lattice Boltzmann method on a CUDA computation platform. *International Journal of Heat and Mass Transfer*, **93**: 273–285. doi:10.1016/j.jheatmasstransfer.2015.09.059.
- Tayebi T, Oztop HF. 2025. Investigation of the Local thermal Non-Equilibrium (LTNE) effects on magneto-natural convection of nano-encapsulated PCMs in an elliptical non-Darcian porous annulus. *International Journal of Heat and Fluid Flow*, **112**: 109710. doi:10.1016/j.jheatfluidflow.2024.109710.
- Wang CY, Mobedi M. 2020. A comprehensive pore scale and volume average study on solid/liquid phase change in a porous medium. *International Journal of Heat and Mass Transfer*, **159**: 120102. doi:10.1016/j.jheatmasstransfer.2020.120102.
- Wang CY, Mobedi M. 2020. A new formulation for nondimensionalization heat transfer of phase change in porous media: An example application to closed cell porous media. *International Journal of Heat and Mass Transfer*, **149**: 119069. doi:10.1016/j.jheatmasstransfer.2019.119069.
- Wang CY, Mobedi M, Kuwahara F. 2019. Analysis of local thermal non-equilibrium condition for unsteady heat transfer in porous media with closed cells: Sparrow number. *International Journal of Mechanical Sciences*, **157–158**: 13–24. doi:10.1016/j.ijmecsci.2019.04.022.
- Wang C, Mobedi M, Kuwahara F. 2019. Simulation of heat transfer in a closed-cell porous media under local thermal non-equilibrium condition. *International Journal of Numerical Methods for Heat & Fluid Flow*, **29**(8): 2478–2500. doi:10.1108/HFF-07-2018-0368.
- Wang CY, Zheng XH, Zhang T, Chen HS, Mobedi M. 2022. The effect of porosity and number of unit cell on applicability of volume average approach in closed cell porous media. *International Journal of Numerical Methods for Heat & Fluid Flow*, **32**(8): 2778–2798. doi:10.1108/HFF-08-2021-0527.
- Zhang YH, Jiang QM, Tan QX, Liu Y, Zhu JJ, Wang JL. 2024. Numerical analysis on heat transfer of porous wick flat micro heat pipe under various operating conditions. *International Communications in Heat and Mass Transfer*, **157**: 107842. doi:10.1016/j.icheatmasstransfer.2024.107842.